Microscopic agents programmed by DNA circuits

Guillaume Gines, A Zadorin, J.-C S Galas, T S Fujii, A S Estevez-Torres, Y Rondelez

Microscopic agents programmed by DNA circuits.

G. Gines[1], A. Zadorin[2,3], J.-C Galas[3], T. Fujii[1], A. Estevez-Torres[2], Y. Rondelez[1,3]**

1. LIMMS, CNRS/Institute of Industrial Science, UMI 2820, University of Tokyo, 153-8505 Tokyo, Japan. **2.** Laboratoire Jean Perrin, CNRS/Université Pierre et Marie Curie, UMR 8237, 4 place Jussieu, 75005 Paris, France. **3.** Laboratoire Gulliver, CNRS/Ecole Supérieure de Physique et Chimie Industrielles, UMR 7083, 10 rue Vauquelin, 75005 Paris, France.

**email : yannick.rondelez@espci.fr

Abstract

Information stored in the sequence of synthetic nucleic acids can be used *in vitro* to create complex reaction networks implementing precisely programmed chemical dynamics. We report here the extension of this approach to program the local and individual chemical behavior of microscopic "agents" dispersed in an enzymatic solution. Agents possess multiple stable states, thus maintaining a memory, and communicate by emitting various orthogonal signals and sensing the behavior of neighboring agents. We build on these elements to create collective behaviors involving thousands of different agents, for example retrieving information over long distances, or creating spatial patterns. This approach recapitulates some fundamental mechanisms of distributed decision making and morphogenesis among living organisms. The possibility to scale up the information-processing capability of DNA-encoded artificial systems could also find applications where many individual clues need to be combined to reach a decision, e.g. in molecular diagnostics.

Molecular programming (MP) holds that information can be processed using molecules as carriers and chemical reactions as computational primitives. In the last decade, this emergent field has crafted an array of molecular mixtures that indeed behave as *systems*, in the engineering sense, even if they are essentially amorphous chemical soups[1,2]. Many of these man-made systems are inspired by existing information-processing molecular networks observed within single cells: logic circuits seen in signaling cascades[3,4]; circadian oscillators pacing the metabolism of light-harvesting microorganisms[5,6]; all-or-nothing switches embedded in genetic regulation pathways[4,7,8], shape-forming morphogen fronts in developing embryos[9–12], etc.

In many cases, however, biological behaviors result from the collective dynamics of many cells exchanging molecular information. Bacteria use quorum sensing to collectively select survival strategies[13,14], multiple cells within embryos exchange morphogens to generate sharp differentiated clusters[15,16], and unicellular organisms such as *Dictyostelium* switch to a multicellular lifestyle to overcome adverse conditions[17].

In this work, we introduce an experimental approach combining existing solution-phase, well-mixed MP techniques and solid-phase DNA biochemistry to create programmable individual microscopic objects. Each particle carries a stable set of DNA instructions controlling its dynamical behavior. It is also able to interact with its neighbors using diffusible signals, providing a way to design collective behaviors involving thousands of -possibly different- agents.

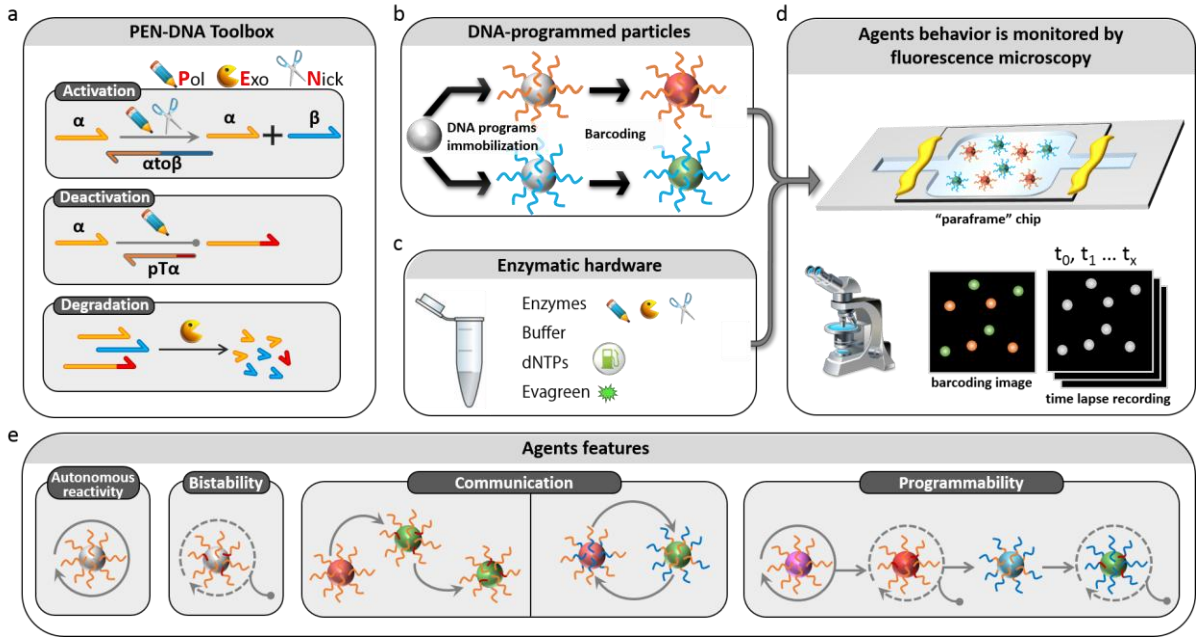

Figure 1. Programming microscopic agents using DNA-encoded reaction rules*. **a**, The PEN DNA toolbox is a set of generic modules that can be cascaded to build molecular programs processed by an enzymatic machinery. **b**, In this study, we convert the solution-phase system to a spatially discrete architecture by attaching the rule-encoding templates to micrometric particles. Particles are barcoded to be easily distinguished by fluorescence according to the set of templates they carry. **c**, The reaction mix contains the enzymatic hardware in addition to the buffer, the fuel dNTPs and a double strand-specific dye EvaGreen. **d**, Particles are incubated in a 2-dimensionnal micro-chamber and the reaction (creation of output) is monitored by microscopic imaging of the EvaGreen fluorescence signals, reflecting the relative amount of active (i.e. double-stranded) templates on each particle. In the case of mixed populations, barcode channels are used to identify the circuit carried by each particle. **e**, Programmed particles behave as independent microscopic agents displaying features such as bistability, communication and programmability.*

We build on the Polymerase/Exonuclease/Nickase Dynamic Network Assembly (PEN DNA) toolbox[5,18], a molecular programming scheme where short oligodeoxyribonucleotides (templates) encode the connectivity information of a network of activating/inhibiting interactions (Fig. 1a). We attach these rule-encoding DNA templates to micrometric porous particles (Fig. 1b). The particles are then immersed within a solution containing the PEN enzymes, leading to the interpretation of the particle-bound DNA rule into a local chemical behavior (Fig. 1c-d). We show that the individual behavior of a bead carrying a tethered PEN DNA network qualitatively reproduces the one observed for solution-phase systems with the same set of templates. However, production of DNA signals is now spatially constrained to the position of the bead, while degradation extends to the bulk of the solution, resulting in the generation of concentration gradients around each agent (Supplementary Notes 1). This creates autonomous, mono- or multi-stable particles that communicate locally through diffusive exchange of signals (Fig. 1e).

These building blocks enable the rational molecular programming of population-scale phenomena[19,20]. We generate spatially random arrays containing thousands of particles in which we observed the propagation of bistable travelling fronts, or the generation of stationary symbiotic activation patterns, depending on the molecular instructions carried by the microscopic agents. We also show that multiple orthogonal layers of chemical communication can be used in a single system. We used this capability to build an assembly where discrete agents cooperate to propagate chemical information over a distance of a few millimeters, check for the presence of a particular bead type, and carry this information back to the origin of the query (Fig. 1e, right).

Particles encoded with a positive feed-back loop (PFL) program

The dynamics of PEN DNA systems, relies on a generalist enzymatic machinery that drives the exchange of DNA signals between the rule templates: a DNA-polymerase elongates an input strand that hybridizes on the input (3') side of a matching template; a nickase recognizes and cuts the resulting full duplex, releasing both the input and a new output DNA. The exonuclease non-specifically degrades all unprotected oligonucleotides (templates are protected), maintaining the system in a responsive out-of-equilibrium state. In functional terms, hybridization and enzymatic reactions collaborate to generate a set of basic modules that can be cascaded in dynamic circuits whose parameters are linked to kinetic, thermodynamic and concentration values. This versatile system has already allowed the construction of various solution-phase circuits such as oscillators[5] or multistable switches[8].

We investigated the possibility of grafting rule-encoding PEN DNA templates onto solid supports in order to create spatially localized DNA programs[21,22] (see Supplementary Information Methods section, all sequences are given in Supplementary Table 1). At first, streptavidin-conjugated porous microparticles (Ø = 34±10 µm) were conjugated to a biotin-modified template αtoα, a dual-repeat sequence catalyzing the positive feedback loop (PFL) reaction α →2α (Fig 2a). Details concerning the properties of the conjugated particles are given in Figures S1-4. These PFL-encoded particles ($P\alpha_M$) were transferred to a master mix containing PEN enzymes, dNTPs and incubated in a flat microscopy chamber. The amplification reaction is monitored using a double strand specific dye (EvaGreen) that fluoresces upon binding the active templates producing the α strand. Time lapse fluorescence imaging revealed the expected behavior for the PFL circuit: an initial exponential amplification phase is followed by a steady-state plateau (production balances diffusion and degradation), then a return to the baseline after exhaustion of dNTPs (Fig. 2c and Supplementary Movie M1).

Diffusion cone + theory…

We first validated biotin modifications as a tethering strategy (Fig S1-2). We grafted femtomoles (billions of copies) of biotinylated template oligonucleotides to streptavidin-modified porous beads

with a diameter of 34±10 µm. When the particles where grafted below their binding capacity, we observed a shell-like geometry and negligible exchange of strands between the beads (Fig. S3-4). We then used standard PEN DNA rules[5,18] to create a biotin-modified template αtoα, a dual-repeat sequence catalyzing the Positive Feedback Loop (PFL) reaction α →2α (Fig 2a). Particles encoded with this strand were transferred to a master mix containing PEN enzymes and dNTPs and incubated in a flat microscopy chamber. Time lapse fluorescence imaging revealed the expected behavior for the PFL circuit: an initial exponential amplification phase is followed by a steady-state plateau (production balances diffusion and degradation), then a return to the baseline after exhaustion of dNTPs (Fig. 2c and Supplementary Movie M1). This behavior closely parallels the one observed for the case of freely diffusing templates (Fig. 2b). In the case of particle-tethered templates however, change in fluorescence signal is observed only on the beads and not in the bulk of the solution, showing that production is indeed localized. The particles also acted in synchrony, suggesting that diffusion of signal strands and/or fuel can mediate communication.

The dimensionless Damköhler number *Da* gives an estimation of the importance of local versus global effects in chemical systems. Here the *Da* associated to grafted particles is much greater than 1 (details of the estimation of *Da* and reaction-diffusion length scales are given in Supplementary Note 2), so we expect a dominance of local effects. Ultimately, a single particle performing an autocatalytic reaction should be able to conserve alone (on its own) a high production of output, despite being constantly depleted by diffusion. To check this self-sustained reactivity, a unique particle was incubated in a large chamber (volume ratio of 10^{-6}, Fig. 2d). Here, the total amount of template would be too small to sustain amplification in a bulk solution (~ 3 fmol for a total volume of 10 µL, i.e. less than one nanomolar). The strands are however highly concentrated within the particle, and we did observe a sharp localized amplification. The following plateau in fluorescence level was sustained for more than 18 hours, indicating that dNTP consumption by the single particle was limited. Amplification and homeostasis are therefore individual properties of particles bearing autocatalytic circuits, and not a global feature of the heterogeneous mixture.

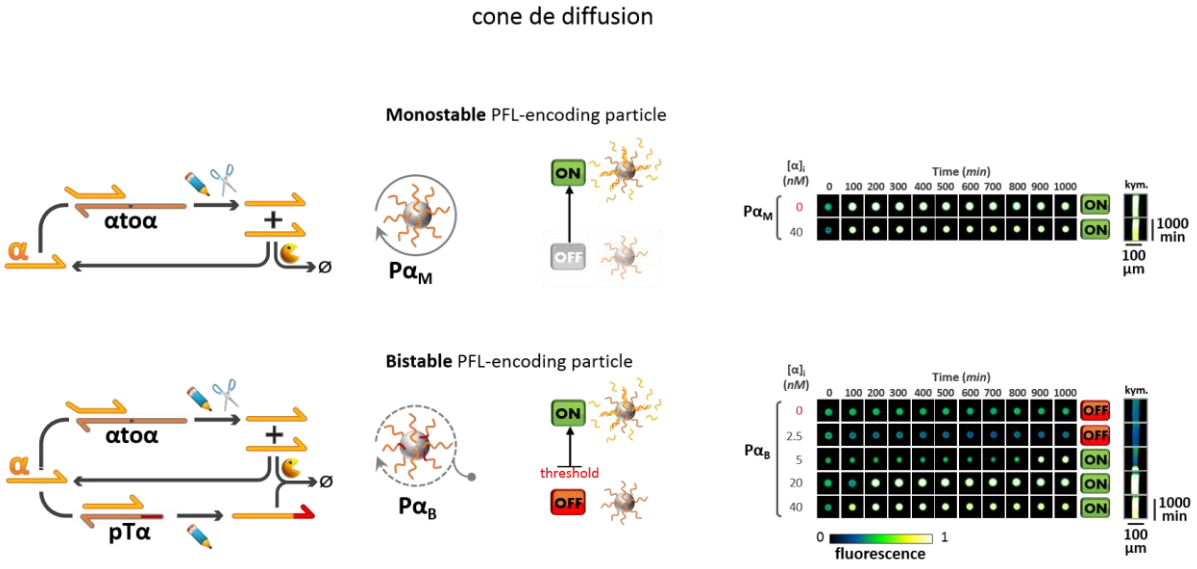

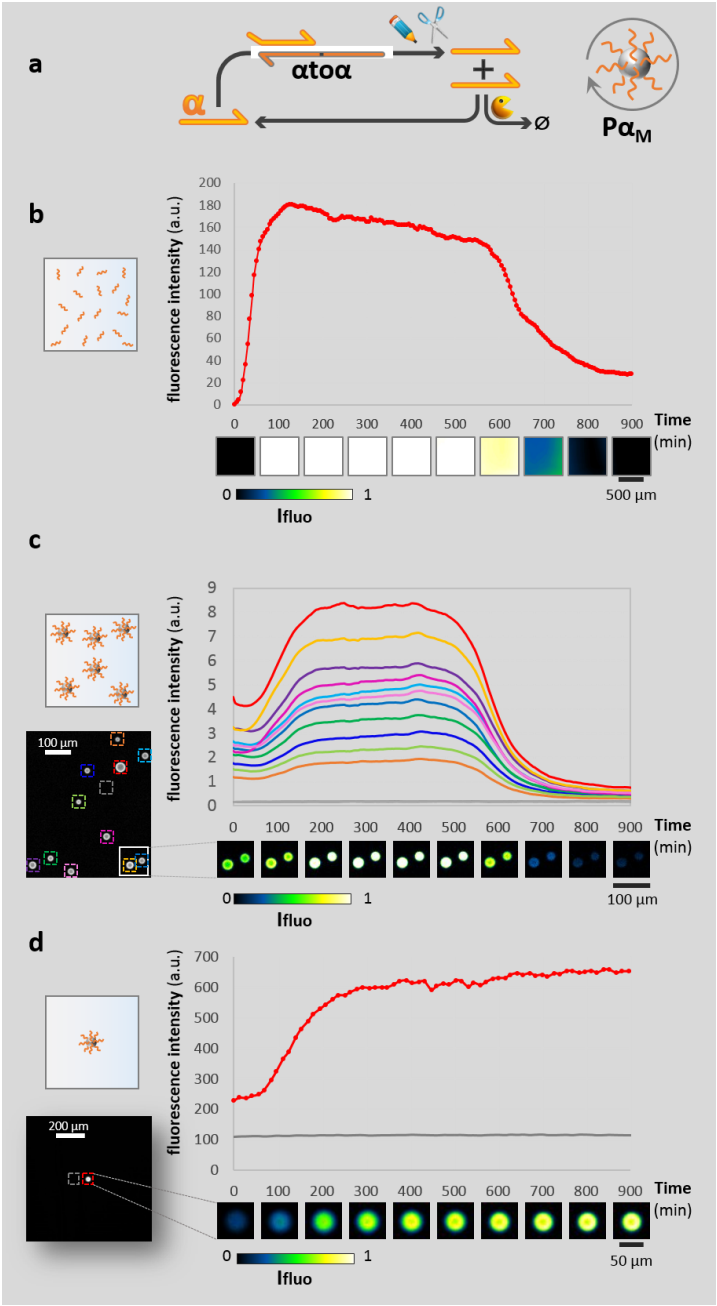

Figure 2. Agents carrying positive feedback templates are autonomous. ***a****, A PFL encoded by template* αtoα *catalyzes the self-activated production of strand* α. ***b, c, d****, Microscopic fluorescence recording of the reaction in a flat micro-chamber in absence of initial trigger α for:* ***b****, freely diffusing templates (conjugated to streptavidin);* ***c****, Multiple microscopic porous particles functionalized with the template* αtoα*;* ***d****, A single particle (particle to chamber volume ratio is 1 : 10^6). The amplification reaction is monitored with a double strand specific dye that fluoresce upon binding to the –double-stranded-active template.*

Bistable agents

In the cases described so far we observed that, even in the absence of initial trigger, particles carrying sufficient αtoα inevitably self-activate after a short period of incubation. This phenomenon is again consistent with the behavior reported for solution-phase amplification systems: autocatalytic templates self-start after some time[23]. This is inherent to the monostability of the first-order PFL network enforced by the dual repeat template: any small perturbation, such as leaky (primer-independent) polymerization of a single output strand is enough to take the system away from the 0 state and initiate exponential amplification. This phenomenon hampers the study of spatial communication between agents because there is only a limited time during which a PFL-bearing particle can wait for a triggering signal without self-activating itself.

In order to stabilize the "OFF" state (corresponding to a non-productive state) we use a species-specific deactivation template (pseudo-template, pT) that catalyzes the addition of a short 3' tail (extension) to the trigger of the associated template (Fig. 3a). Like the autocatalytic template the

pseudo-template is composed of a 3' input binding part, but its output part consists of only a few nucleotides (poly-dA or poly-dT). As the trigger binds to the pT, it is elongated by the polymerase. The resulting extended strand slowly melts away (regenerating the pseudo-template so that this mechanism is catalytic) and is now unable to prime further reactions. This mechanism (Fig. S5) constitutes a signal-specific sink of tunable throughput that has been used to build multistable and excitable circuits[24]. We adapt this strategy to particle systems by co-immobilizing the autocatalytic template with the corresponding pseudo-template on the particles.

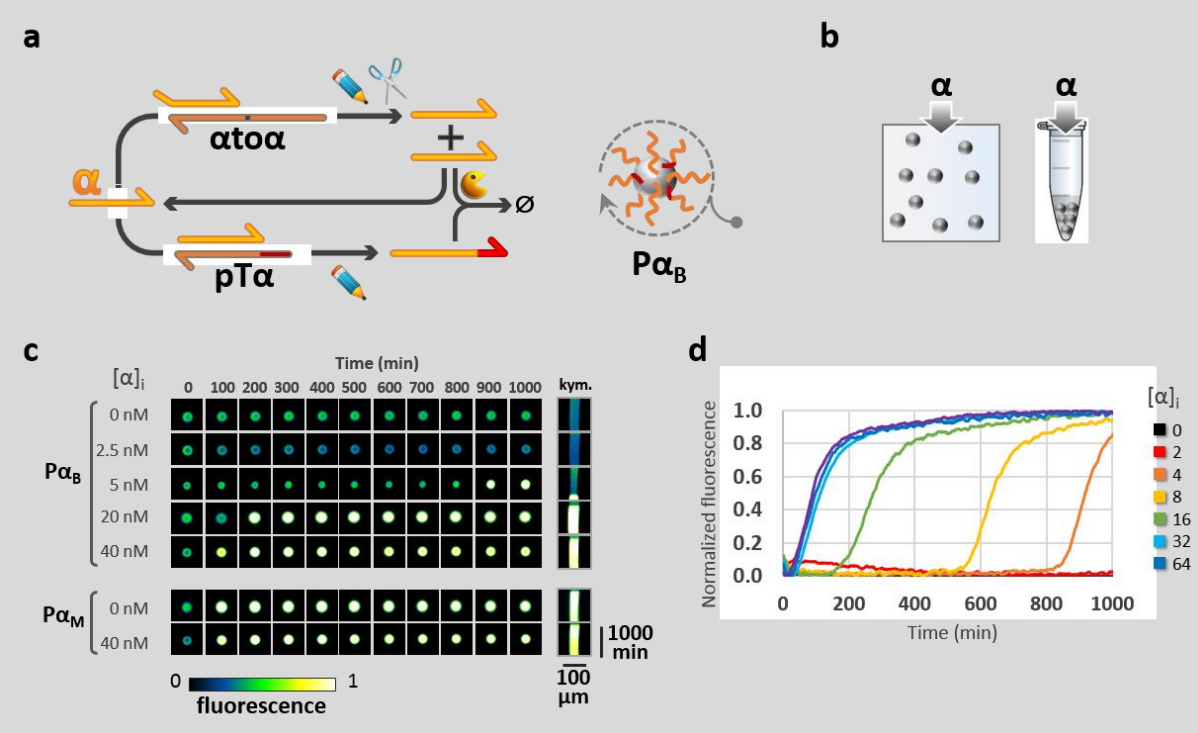

***Figure 3. Construction of 2-state agents using a bistable molecular program**. **a**, Bistable design based on a fast but saturable deactivation pathway targeting the autocatalytic species α. The two ~~encoding~~ templates (αtoα and pTα) are co-grafted on beads to obtain bistable agents ($Pα_B$). **b**, Experimental setup: real-time signal is recorded either by fluorescence microscopy within 2D chambers or in test tubes (beads pellet) using a thermocycler. **c**, Panel of snapshots extracted from time-lapse fluorescence recording of individual particles $Pα_B$ incubated with various initial amounts of α strand ($0 \leq [α] \leq 40$ nM). The rightmost image shows the reconstructed kymogram. **d**, Fluorescence time traces of test tubes containing ≈ 800 $Pα_B$ in 10 µL, triggered with various concentrations of strand α.*

Microscopy (Fig. 3c) and bulk (Fig. 3d) experiments show that co-grafted particles now possess two different stable states (nonproductive and productive, referred as the "OFF" and "ON" states) which are selected depending on the initial conditions (respectively high or low trigger). Pseudo-templates are therefore able to abolish self-start, even in the context of the very high local concentration of templates (~ 250 µM in the bulk of the sphere). If no signal is present in their environment, the particles stay in their OFF state so that the activation of bistable beads necessarily relies on the application of a stimulus exceeding a given threshold. In the following, we call the particles carrying only the autocatalytic template $Pα_M$ and the co-grafted particles $Pα_B$ (M and B stand for monostable and bistable, respectively).

Monostable and bistable particle encoded with a positive feedback loop

The dynamics of PEN DNA systems, relies on a generalist enzymatic machinery that drives the exchange of DNA signals between the rule templates: a DNA-polymerase elongates an input strand

that hybridizes on the input (3') side of a matching template; a nickase recognizes and cuts the resulting full duplex, releasing both the input and a new output DNA. The exonuclease non-specifically degrades all unprotected oligonucleotides (templates are protected), maintaining the system in a responsive out-of-equilibrium state. In functional terms, hybridization and enzymatic reactions collaborate to generate a set of basic modules that can be cascaded in dynamic circuits whose parameters are linked to kinetic, thermodynamic and concentration values. This versatile system has already allowed the construction of various solution-phase circuits such as oscillators[5] or multistable switches[8].

We investigated the possibility of grafting rule-encoding PEN DNA templates onto solid supports in order to create spatially localized DNA programs[21,22] (see Supplementary Information Methods section, all sequences are given in Supplementary Table 1). At first, streptavidin-conjugated porous microparticles (Ø = 34±10 µm) were conjugated to a biotin-modified template αtoα, a dual-repeat sequence catalyzing the positive feedback loop (PFL) reaction α →2α (Fig 2a). Details concerning the properties of the conjugated particles are given in Figures S1-4. These PFL-encoded particles were transferred to a master mix containing PEN enzymes, dNTPs and incubated in a flat microscopy chamber. The amplification reaction is monitored using a double strand specific dye (EvaGreen) that fluoresces upon binding the active templates producing the α strand. Time lapse fluorescence imaging revealed the expected behavior for the PFL circuit: an initial exponential amplification phase is followed by a steady-state plateau (production balances diffusion and degradation), then a return to the baseline after exhaustion of dNTPs (Fig. Sx and Supplementary Movie M1). This behavior closely parallels the one observed for the case of freely diffusing templates (Fig. Sx). In the case of particle-tethered templates however, change in fluorescence signal is observed only on the particle position and not in the bulk of the solution. Therefore, the production of the output α is now localized while its degradation by the exonuclease is likely to occur in the whole chamber. To assess the concentration profile of α, a few autocatalytic particles are displayed in a chamber together with particles functionalized by the template αtoβ, acting like a sensor of the α strand: upon reversible binding of the input strand, these particles produce an inert β strand. The reaction is monitored using EvaGreen as reporter of the overall activity of each particle.

Diffusion cone + theory…

Notwithstanding the absence of initial trigger, particles carrying the template αtoα inevitably switch to the "ON" state after a short period of incubation (Fig. XX and Fig. 2b). This phenomenon is again consistent with the behavior reported for solution-phase amplification systems: autocatalytic templates self-start after some time because the first-order PFL network enforced by the dual repeat template is intrinsically monostable.[23] In order to stabilize the "OFF" state (corresponding to a non-productive state) we use a species-specific deactivation template (pseudo-template, pT) that catalyzes the addition of a short 3' tail (extension) to the trigger of the associated template (Fig. 2c). Like the autocatalytic template the pseudo-template is composed of a 3' input binding part, but its output part consists of only a few nucleotides (poly-dA or poly-dT). As the trigger binds to the pT, it is elongated by the polymerase. The resulting extended strand slowly melts away (regenerating the pseudo-template so that this mechanism is catalytic) and is now unable to prime further reactions. This mechanism (Fig. S5) constitutes a signal-specific sink of tunable throughput that has been used to build multistable and excitable circuits[24]. We adapt this strategy to particle systems by co-immobilizing the autocatalytic template with the corresponding pseudo-template on the particles. Microscopy (Fig. XX) experiments show that co-grafted particles now possess two different stable states (nonproductive and productive, referred as the "OFF" and "ON" states) which are selected depending on the initial conditions (respectively high or low trigger concentration). Pseudo-templates are therefore able to abolish self-start, even in the context of the very high local concentration of templates (~ 250 µM in the bulk of the sphere). If no signal is present in their

environment, the particles stay in their OFF state so that the activation of bistable beads necessarily relies on the application of a stimulus exceeding a given threshold. In the following, we call the particles carrying only the autocatalytic template $P\alpha_M$ and the co-grafted particles $P\alpha_B$ (M and B stand for monostable and bistable, respectively).

Communication: travelling front propagation in a population of bistable agents

We then moved on to evaluate the communication capabilities between these independent agents. Figure 4a depicts an experiment where bistable particles $P\alpha_B$, initially in their OFF state, are randomly positioned in an extended channel roughly one centimeter long. On one side of the channel, dye-barcoded monostable particles $P\alpha_M$ (without pseudo-template) are introduced (Fig. 4b). As expected, $P\alpha_M$ particles self-activate after a short delay. The concentration inhomogeneity that they create is strong enough to trigger the switching of neighboring $P\alpha_B$, which in turn lights up and propagates the signal to other bistable particles (Fig. 4c-d and Supplementary Movie M2). This generates a travelling front that gradually converts all particles in the channel. Switch-on times for $P\alpha_B$ particles correlate linearly to the distance from the monostable triggering beads (Fig. 4e).

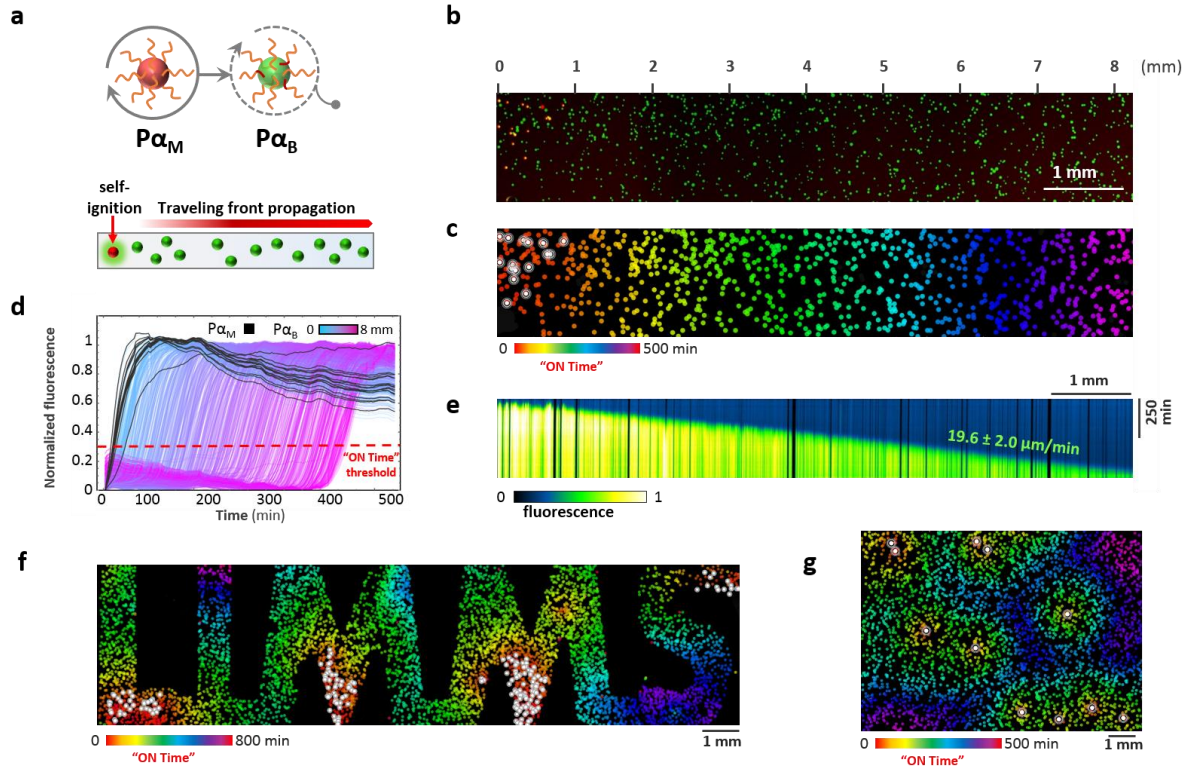

Figure 4. Travelling front propagation across a population of bistable agents ($P\alpha_B$). ***a****, Schematic representation showing the propagation of an activation signal triggered initially by the self-ignition of monostable agents ($P\alpha_M$).* ***b****, Barcode image (red spots = $P\alpha_M$; green dots = $P\alpha_B$).* ***c****, Colorized representation of the front propagation where color represents the time of amplification ("ON" time) for each particle. ~~The top bar indicates the longitudinal~~The white dots indicate the positions of the $P\alpha_M$ (red stripes).* ***d****, Fluorescence time traces extracted for each particle show the spontaneous switching of monostable particles and the correlation between the position of bistable particles and their amplification start time.* ***e****, The kymogram reveals the constant velocity of the travelling front across the population of $P\alpha_B$. f,g, Traveling front propagation across population of $P\alpha_B$ in various geometric environments. For details on image processing see Fig. S10.*

~~It is noteworthy that the front velocity is much lower than it would be if the templates and pseudo-templates where free and homogeneously distributed in the solution (Fig. S6). Indeed, production occurs only at the particle's position, on non-diffusing templates, while the degradation of diffusing signal happens in the whole chamber (thus limiting the amount of triggers able to diffuse from bead to bead).~~ The velocity of the front propagation can be finely tuned between a few to tens of micrometers per minute by tinkering with the agents' features (ratio template/pseudo-template, Fig. S7) or the experimental conditions (such as enzymes concentration or particle density, Fig. S8-9). Additionally, these dynamic activation patterns have been generated in various geometric environments (Fig XX).

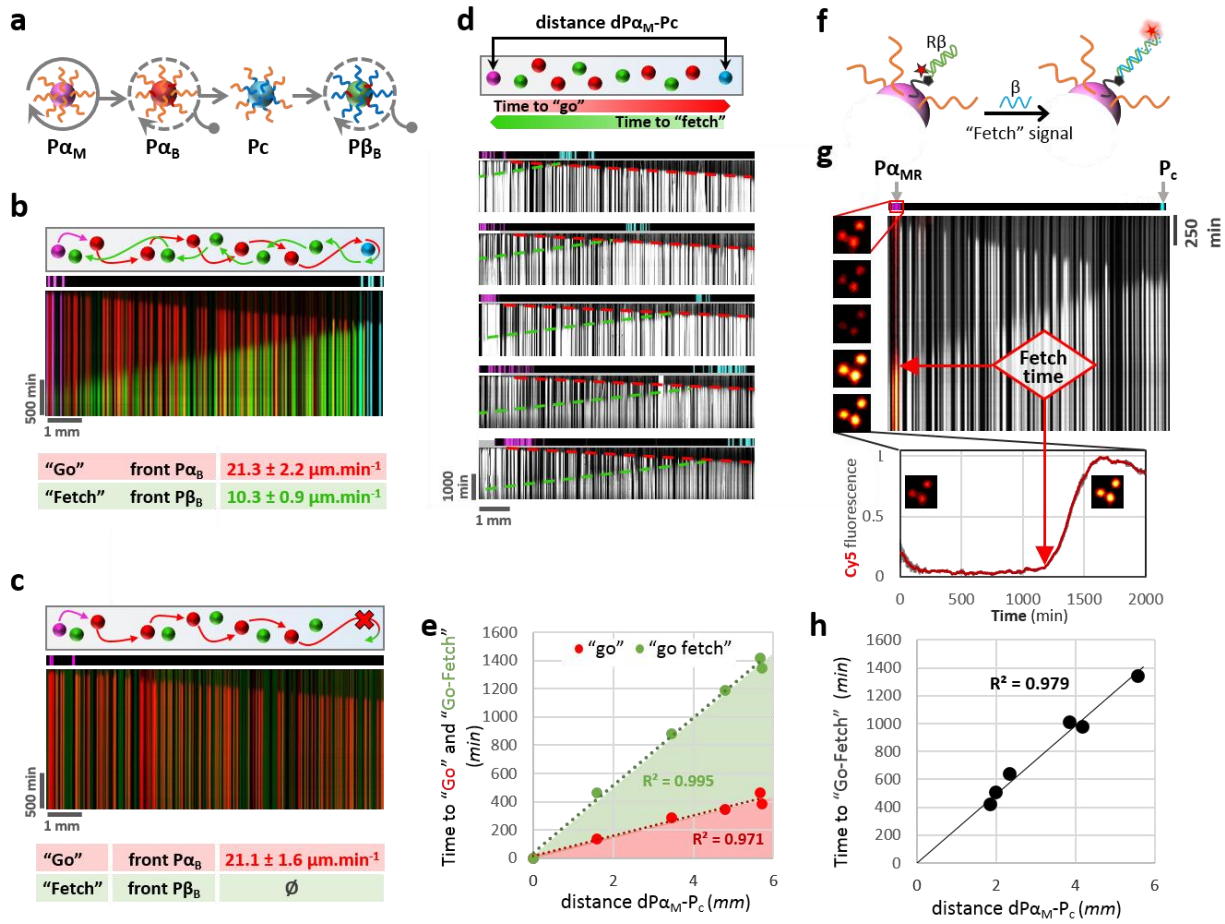

Figure 5. "Go-Fetch" program using 4 agent populations. ***a****, Schematic representation showing the flow of information between the four bead types.* ***b****, Kymogram representation of the experiment. Evagreen fluorescence signals associated with the beads are color-coded according to the bead type (magenta = $P\alpha_M$, red = $P\alpha_B$, cyan = $P_{\alpha\rightarrow\beta}$, green = $P\beta_B$).* ***c****, Control experiment with no converter bead at the end of the channel.* ***d****, Converter beads are positioned at different locations in the channel.* ***e****, Front travelling time as a function of sender-target distance in* ***d****.* ***f****, An additional mechanism allows the sender bead to detect the arrival of the return front.* ***g****, Experimental snapshots, kymogram and plot of the red fluorescence for sender particles.* ***h****, Light-up time of the sender particle as a function of its distance to the nearest converter.*

Programmability: a 4-agent network

Communication between the particles need not be limited to a single molecular pathway: as observed in bacterial quorum sensing, various agents can possess distinct circuits, producing and detecting orthogonal signaling molecules[25]. To demonstrate this concept, we designed a network using two signaling compounds and four different kinds of agents. First, we created a second type of

bistable particles producing and emitting strand β (Fig. S11). We confirmed the orthogonality of the two pathways in travelling front experiments using a mixed population of bistable agents $P\alpha_B$ and $P\beta_B$. α and β fronts were set to propagate in opposite directions, and affected only the corresponding particles (Fig. S12). In a second step, the initiation of the front propagating through the $P\beta_B$ population was coupled to the arrival of the front producing α (Fig. 5a), using converter particles $P_{\alpha\to\beta}$, carrying the template αtoβ (which take α as input to produce β as output). The topography of the spatial network, nicknamed "Go-Fetch", is as follows: bistable agents $P\alpha_B$ and $P\beta_B$ are mixed together in a channel. At one extremity, a few monostable $P\alpha_M$ (the sender particles) are deposited; on the opposite side of the channel, the converter agents $P_{\alpha\to\beta}$ represent the target. Figure 5b (see also Fig. S13 and Supplementary Movie M3) shows sequentially i) the self-activation of the monostable beads $P\alpha_M$, ii) the propagation of the signal through the bistable population $P\alpha_B$, iii) the activation of the converter particles (which light on once the front reaches their position) and iv) the initiation and propagation of a second front travelling back to the initial sender, through the bistable particles $P\beta_B$.

~~Satisfyingly,~~ A control experiment without converter agents also produced a first front propagation through particles $P\alpha_B$, but the return front was not generated and all particles $P\beta_B$ stayed "OFF" for the duration of the experiment (30 hours). These results demonstrate the use of multiple speciated agents collaborating in a unique, spatially and time-resolved task. This program can for example be used by a sender particle to infer its distance to the nearest target particle, over a scale that is 3 orders of magnitude larger than the agents themselves. By arbitrarily varying the position of the $P_{\alpha\to\beta}$ in the channel, we indeed observed that the sender particle receives this distance information as the time needed for the signal to return, with a linear relationship between distance and time (Fig. 5d-e). It is possible to imagine that the particles use this "chemical sonar" to control downstream processes ... As a basic model of differentiation, we added a module to the sender particles so that they light up as soon as the system has fetched the distance information (Fig. 5f): $P\alpha_M$ are modified with a molecular beacon-like probe, which fluoresces upon binding and polymerization of the returning β strands (Fig. 5g). The full system now differentiates the sender particles $P\alpha_M$ with a timing that is precisely controlled by their position relative to the nearest converter particles $P_{\alpha\to\beta}$ (Fig. 5h)[15].

One may note that the return front is much slower than the first front passing through $P\alpha_B$. It is also twice slower than the propagation through $P\beta_B$ initiated by $P\beta_M$ (Fig. S13), demonstrating that this is not due to the $P\beta_B$ propagation system itself being intrinsically slower. We therefore conclude that it is the presence of *active* $P\alpha_B$ that slows down the propagation of the β front. This observation suggests that competition for catalytic resources, such as nickase and/or polymerase, happens even if the two networks are spatially separated and occupy only a minor fraction of the total enzymatic mixture[26,27] (see also Fig. S9). Competition/depletion/concentration enzymes ???

Colony formation by symbiotic particles

While the previous experiments show that beads can behave as independent entities, it is also possible to engineer synergic dependency and cooperativity among the individual agents. To evaluate this possibility, we split an autocatalytic loop into two templates (one encoding γtoδ and one δtoγ), which are separately attached to different microspheres (Fig. Xa). An active PFL network now necessarily requires oligonucleotides to be exchanged between both bead types. We created flat fluidic chambers containing a high density of $P_{\gamma\to\delta}$ particles (10^5 part./cm^2) and a few $P_{\delta\to\gamma}$ particles (Fig. XXb). Real-time fluorescence monitoring revealed the emergence of localized activation colonies located around the minority particles (Figure 6Xc, S15 and Supplementary Movie M4). These colonies emerge and grow to reach a steady state (Figure 6Xd). The activity within the majority population is directly related to the presence of a minority bead in their neighborhood. . The steady state fluorescence of the majority beads decays quickly with the distance to their feeding $P_{\delta\to\gamma}$, and fitting yield a characteristic length on the order of 50 µm (Fig. XXe, see Supplementary

Note 3 for justification of the exponential decay model). Interestingly, we observe anisotropy in the particle reactivity, the side of the $P_{\gamma\rightarrow\delta}$ exposed to the $P_{\delta\rightarrow\gamma}$ being more active (Fig. Xd) at steady state ?. This confirms that the system dissipate enough free energy to maintain strong steady-state gradients over micrometric (~ 10 um) distances.(in the absence of a active sustaining mechanism such gradient woule equilibrate in r^2/D = xx minute)

In the experiment depicted in Figure XX, we gradually increased the density of minority particles from XX to XX part./cm^2. At low $P_{\delta\rightarrow\gamma}$ densities (XX to XX part.cm^2), the colonies are small, well defined, and similar for all conditions. However, when the density of minority beads reaches a threshold, we observe a sudden increase in colony size and much more activity in the population of majority beads. Since this happens when the mean distance between minority beads becomes close to the colonies characteristic length, it suggests that a colony-to-colony cooperation activation mechanism comes to play, where the signal strand diffusing from one colony is able to activate majority beads from a second colony, reinforcing it, and beneficiating in return. We therefore observe a ~~double~~ two-tier communication mechanism where $P_{\gamma\rightarrow\delta}$ beads locally detect the presence of a minority bead in their vicinity, but also globally sense the average density of the minority partners through a percolation mechanism associated with a sharp density threshold.

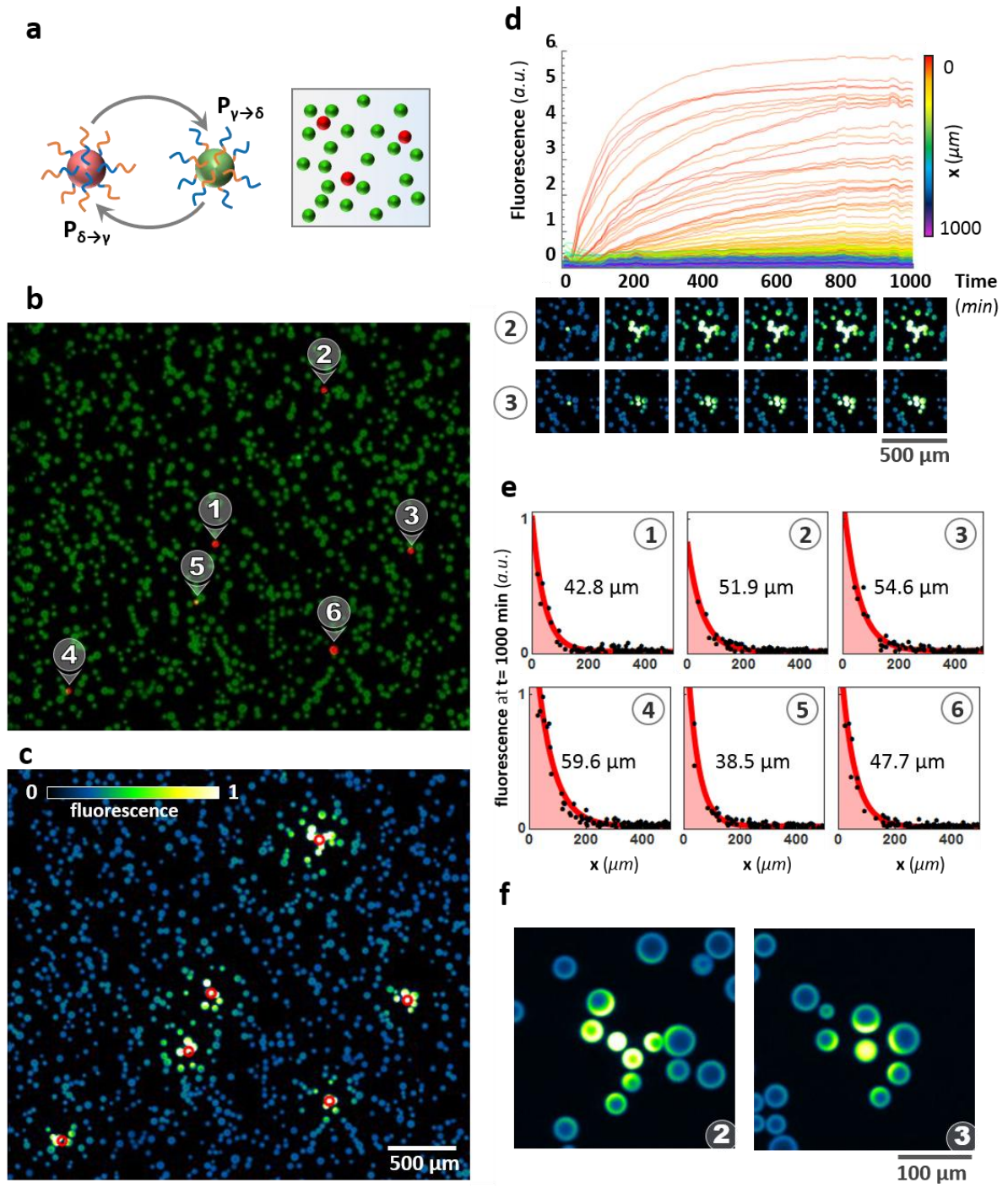

Figure 6. Mixed populations of symbiotic particles form localized clusters of activity around the minority agents. ***a****, Schematic representation of the system.* ***b****, Barcode image of a portion of the fluidic chamber (Green = $P_{\gamma\to\delta}$, Red = $P_{\delta\to\gamma}$. c, Snapshot image of EvaGreen fluorescence at t = 1000 min. The minority particles are indicated by red circles.* ***d****, The fluorescence of each majority particle is plotted as a function of its distance to the nearest minority particle. The bottom images represent fluorescence snapshots of two colonies at the corresponding time.* ***e****, Profile of reactivity for each colony. The fluorescence of each majority particle is plotted as a function of its distance to the minority particle and fitted with a simple exponential decay (length parameters l_d are indicated in black).* ***f****, Confocal image (10X magnification) of two colonies showing the anisotropy of reactivity for the surrounding majority particles.*

~~***Figure 6. Mixed populations of symbiotic particles form localized clusters of activity around the minority agents. a,*** *Schematic representation of the system.* ***b,*** *Snapshot of a portion of the fluidic chambers at t = 300 min. The minority particles (indicated by red crosses) are present at increasing concentrations in the various experiments (their total number in each chamber is given in parenthesis).* ***c,*** *Time lapse images for the two labelled clusters in chamber #4 and #5. Images are taken every 30 minutes.* ***d,*** *Profile of activity for two clusters from chamber #4. The fluorescence of each majority bead is plotted as a function of its distance to the minority particle and fitted with a simple exponential decay (length parameters are 100 (top) and 63 µm (bottom)). The inset shows the corresponding cluster.* ***e,*** *Plot of the mean distance between two minority particles and the activity that they generate among the majority particles, for various densities of minority particles. The activity is defined as the number of majority particles which cross a threshold of fluorescence.*~~

Conclusion

Communication using diffusive compounds is a general biological strategy to build multi-agents behaviors at microscopic scales. Diffusive cell signaling is typically classified into autocrine (self-communication) or paracrine signaling (cross-communication)[28]. These two types are naturally implemented in our system because the encoding templates can be designed to use either endogenous, exogenous or both signals as inputs.

To better understand the scaling associated with the usage of diffusive communication between agents, we analytically solved the concentration profile generated by the shell-like reacting particles (Supplementary Note 4). The mathematical expression depends on the dimensionality of the problem[29], but the length parameter is always controlled by $\sqrt{D/k}$, where D is the diffusion rate and k the first-order degradation rate for the signaling compound. In our conditions, these parameters are D = 18.10^3 µm^2.min^{-1} and k =0.5 min^{-1}, which predicts a length scale of 200 µm, in agreement with our observations (Fig. 5d and Supplementary Note 3). A particle thus communicates efficiently with a neighborhood that is one order of magnitude larger than its size, enabling the unfolding of collective behaviors over relatively large distances.

Our strategy to give memory and differentiated states to the agents involves autocrine bistable circuits based on PFL[30,31]. In the absence of physical boundaries, this approach requires that each particle is able to ~~autonomously~~ maintain its high state, i.e. compensate for the signals lost by diffusion. Solving the previous source and decay model in the case of an isolated particle carrying a positive feedback loop exposes the experimental requirements (Supplementary Note 4 and 5): our model predicts the existence of a critical size, or critical grafting density, below which a particle loses the ability to maintain a differentiated state. In other words, competition between global and local effects imposes that smaller agents dissipate faster in order to maintain their individuality.

Such competition between global and local effects has already been pointed out for other tethered DNA systems[32] and imposes constraints on the miniaturization of molecular programming approaches. Compartmentalization techniques, such as microfabricated chambers, vesicles or emulsions[33] provide an alternative to direct tethering of the DNA rules. Compartments efficiently restrict the diffusion of reactive species[34], but conversely require specific strategies in order to open communication channels between the units[35–38]. Engineered microorganisms have also been used to implement collective behaviors, although the programming of living systems for such tasks remains challenging[39–43].

Our approach based on template-decorated particles provides the basic set of tools required to build and study artificial microscopic communities[19]. *It uses a hierarchical approach that maintains a rational link from molecular pairwise interactions all the way to multi-particles dynamics. Compared to previous work in the study of collective behaviors[45–47], the main advantage is a high level of programmability[44] i.e. that fact that one can freely decide the set of signals to which a given particle is sensitive, and its precise chemical behavior in response to these signals. Our example with the go-fetch network has shown that, like in a multicellular organism, particles carrying different sets of templates can take on the various specialized roles necessary to achieve a global task. The colony*

experiment demonstrates fine sensing of the features of the local and global environment. While the particles used here are too large to display Brownian motion, one may envision that microscopic agents whose motility is controlled by the environment-sensitive network they carry could provide a path to dynamically self-shaping materials. ~~With a straightforward synthesis, they open the route to a massive scale-up in the complexity of man-made molecular computing systems. In particular, they will bring a high level of programmability to the study of collective behaviors, and the modelling of biological morphogenesis.~~ In practical diagnostic applications, we also envision that each particle could be programmed to independently perform a different sensing task, while collaborating with the others to provide a global consensus decision[4].

Methods

Methods and associated references are available in the **Supplementary files.**

Acknowledgments

This work was supported by the JSPS with a Grant-in-Aid from the JSPS for Scientific Research on Innovative Areas "Synthetic Biology for Comprehension of Biomolecular Networks" (#23119001), and an ERC Consolidator grant "ProFF" (#647275). G.G. acknowledges financial support by the JSPS Postdoc program. We thank Nicolas Bredeche and Nathanael Aubert-Kato and Anthony Genot for advices and Yannick Tauran and Alexandre Baccouche for expressing and purifying the exonuclease. Correspondence should be sent to Y.R. (yannick.rondelez@espci.fr)

Author contributions

G.G. designed the study, performed experiments, analyzed the data and wrote the manuscript. A.Z. did mathematical analysis, contributed to image analysis and manuscript writing. J.C.G, A.E.T. contributed to experimental setup and designed the study. T.F. provided support with the microfluidic platform. Y.R. conceived, designed, and supervised the study, analyzed the data and wrote the manuscript.

Additional information

Supplementary information is available for this paper. Reprints and permissions information is available online at …. Correspondence and requests for materials should be addressed to Y.R.

References

1. Padirac, A., Fujii, T. & Rondelez, Y. Nucleic acids for the rational design of reaction circuits. *Curr. Opin. Biotechnol.* **24,** 575–580 (2013).
2. Zhang, D. Y. & Seelig, G. Dynamic DNA nanotechnology using strand-displacement reactions. *Nat. Chem.* **3,** 103–113 (2011).
3. Han, D. *et al.* A cascade reaction network mimicking the basic functional steps of adaptive immune response. *Nat. Chem.* **7,** 835–841 (2015).
4. Chen, Y.-J. *et al.* Programmable chemical controllers made from DNA. *Nat. Nanotechnol.* **8,** 755–762 (2013).

5. Montagne, K., Plasson, R., Sakai, Y., Fujii, T. & Rondelez, Y. Programming an in vitro DNA oscillator using a molecular networking strategy. *Mol. Syst. Biol.* **7,** 466 (2011).
6. Kim, J. & Winfree, E. Synthetic in vitro transcriptional oscillators. *Mol. Syst. Biol.* **7,** 465 (2011).
7. Kim, J., White, K. S. & Winfree, E. Construction of an in vitro bistable circuit from synthetic transcriptional switches. *Mol. Syst. Biol.* **2,** 68 (2006).
8. Padirac, A., Fujii, T. & Rondelez, Y. Bottom-up construction of in vitro switchable memories. *Proc. Natl. Acad. Sci.* **109,** E3212–E3220 (2012).
9. Scalise, D. & Schulman, R. Designing modular reaction-diffusion programs for complex pattern formation. *TECHNOLOGY* **02,** 55–66 (2014).
10. Zadorin, A. S., Rondelez, Y., Galas, J.-C. & Estevez-Torres, A. Synthesis of Programmable Reaction-Diffusion Fronts Using DNA Catalyzers. *Phys. Rev. Lett.* **114,** 068301 (2015).
11. Padirac, A., Fujii, T., Estévez-Torres, A. & Rondelez, Y. Spatial Waves in Synthetic Biochemical Networks. *J. Am. Chem. Soc.* **135,** 14586–14592 (2013).
12. Zambrano, A., Zadorin, A. S., Rondelez, Y., Estevez-Torres, A. & Galas, J.-C. Pursuit-and-evasion Reaction-diffusion Waves In Micro-reactors with Tailored Geometry. *J. Phys. Chem. B* (2015). doi:10.1021/jp509474w
13. Miller, M. B. & Bassler, B. L. Quorum Sensing in Bacteria. *Annu. Rev. Microbiol.* **55,** 165–199 (2001).
14. Waters, C. M. & Bassler, B. L. QUORUM SENSING: Cell-to-Cell Communication in Bacteria. *Annu. Rev. Cell Dev. Biol.* **21,** 319–346 (2005).
15. Pourquié, O. The Segmentation Clock: Converting Embryonic Time into Spatial Pattern. *Science* **301,** 328–330 (2003).

16. Baker, R. E., Schnell, S. & Maini, P. K. A clock and wavefront mechanism for somite formation. *Dev. Biol.* **293,** 116–126 (2006).
17. Kessin, R. H. *Dictyostelium: Evolution, Cell Biology, and the Development of Multicellularity*. (Cambridge University Press, 2001).
18. Baccouche, A., Montagne, K., Padirac, A., Fujii, T. & Rondelez, Y. Dynamic DNA-toolbox reaction circuits: A walkthrough. *Methods* **67,** 234–249 (2014).
19. Yashin, V. V., Kolmakov, G. V., Shum, H. & Balazs, A. C. Designing Synthetic Microcapsules that Undergo Biomimetic Communication and Autonomous Motion. *Langmuir* (2015). doi:10.1021/acs.langmuir.5b01862
20. Taylor, A. F., Tinsley, M. R. & Showalter, K. Insights into collective cell behaviour from populations of coupled chemical oscillators. *Phys. Chem. Chem. Phys.* (2015).
21. Yashin, R., Rudchenko, S. & Stojanovic, M. N. Networking Particles over Distance Using Oligonucleotide-Based Devices. *J. Am. Chem. Soc.* **129,** 15581–15584 (2007).
22. Jung, C., Allen, P. B. & Ellington, A. D. A stochastic DNA walker that traverses a microparticle surface. *Nat. Nanotechnol.* **11,** 157–163 (2016).
23. Tan, E. *et al.* Specific versus Nonspecific Isothermal DNA Amplification through Thermophilic Polymerase and Nicking Enzyme Activities†. *Biochemistry (Mosc.)* **47,** 9987–9999 (2008).
24. Montagne, Kevin, Gines, Guillaume, Fujii, Teruo & Rondelez, Yannick. Creative destruction: Boosting functionality of synthetic DNA circuits with tailored degradation. *Under review.*
25. Davis, R. M., Muller, R. Y. & Haynes, K. A. Can the Natural Diversity of Quorum-Sensing Advance Synthetic Biology? *Front. Bioeng. Biotechnol.* **3,** (2015).

487 26. Genot, A. J., Fujii, T. & Rondelez, Y. Scaling down DNA circuits with competitive neural
488 networks. *J. R. Soc. Interface* **10,** 20130212 (2013).
489 27. Rondelez, Y. Competition for Catalytic Resources Alters Biological Network Dynamics.
490 *Phys. Rev. Lett.* **108,** 018102 (2012).
491 28. Youk, H. & Lim, W. A. Secreting and Sensing the Same Molecule Allows Cells to Achieve
492 Versatile Social Behaviors. *Science* **343,** 1242782 (2014).
493 29. Soh, S., Byrska, M., Kandere-Grzybowska, K. & Grzybowski, B. A. Reaction -Diffusion
494 Systems in Intracellular Molecular Transport and Control. *Angew. Chem. Int. Ed Engl.* **49,**
495 4170–4198 (2010).
496 30. Brandman, O. & Meyer, T. Feedback Loops Shape Cellular Signals in Space and Time.
497 *Science* **322,** 390–395 (2008).
498 31. Wolf, D. M. & Arkin, A. P. Motifs, modules and games in bacteria. *Curr. Opin. Microbiol.*
499 **6,** 125–134 (2003).
500 32. Teichmann, M., Kopperger, E. & Simmel, F. C. Robustness of Localized DNA Strand
501 Displacement Cascades. *ACS Nano* (2014). doi:10.1021/nn503073p
502 33. Hasatani, K. *et al.* High-throughput and long-term observation of compartmentalized
503 biochemical oscillators. *Chem. Commun. Camb. Engl.* **49,** 8090–8092 (2013).
504 34. Toiya, M., González-Ochoa, H. O., Vanag, V. K., Fraden, S. & Epstein, I. R. Synchronization
505 of Chemical Micro-oscillators. *J. Phys. Chem. Lett.* **1,** 1241–1246 (2010).
506 35. Tayar, A. M., Karzbrun, E., Noireaux, V. & Bar-Ziv, R. H. Propagating gene expression
507 fronts in a one-dimensional coupled system of artificial cells. *Nat. Phys.* **11,** 1037–1041
508 (2015).
509 36. Dewey, D. C., Strulson, C. A., Cacace, D. N., Bevilacqua, P. C. & Keating, C. D. Bioreactor
510 droplets from liposome-stabilized all-aqueous emulsions. *Nat. Commun.* **5,** 4670 (2014).

37. Villar, G., Graham, A. D. & Bayley, H. A Tissue-Like Printed Material. *Science* **340,** 48–52 (2013).

38. Weitz, M. *et al.* Communication and Computation by Bacteria Compartmentalized within Microemulsion Droplets. *J. Am. Chem. Soc.* **136,** 72–75 (2014).

39. Lou, C. *et al.* Synthesizing a novel genetic sequential logic circuit: a push-on push-off switch. *Mol. Syst. Biol.* **6,** 350 (2010).

40. Elowitz, M. B. & Leibler, S. A synthetic oscillatory network of transcriptional regulators. *Nature* **403,** 335–338 (2000).

41. Danino, T., Mondragón-Palomino, O., Tsimring, L. & Hasty, J. A synchronized quorum of genetic clocks. *Nature* **463,** 326–330 (2010).

42. Amemiya, T. *et al.* Collective and individual glycolytic oscillations in yeast cells encapsulated in alginate microparticles. *Chaos Interdiscip. J. Nonlinear Sci.* **25,** 064606 (2015).

43. Basu, S., Gerchman, Y., Collins, C. H., Arnold, F. H. & Weiss, R. A synthetic multicellular system for programmed pattern formation. *Nature* **434,** 1130–1134 (2005).

44. Aubert, N., Mosca, C., Fujii, T., Hagiya, M. & Rondelez, Y. Computer-assisted design for scaling up systems based on DNA reaction networks. *J. R. Soc. Interface* **11,** 20131167 (2014).

45. Tinsley, M. R., Taylor, A. F., Huang, Z. & Showalter, K. Emergence of Collective Behavior in Groups of Excitable Catalyst-Loaded Particles: Spatiotemporal Dynamical Quorum Sensing. *Phys. Rev. Lett.* **102,** 158301 (2009).

46. Taylor, A. F., Tinsley, M. R., Wang, F., Huang, Z. & Showalter, K. Dynamical Quorum Sensing and Synchronization in Large Populations of Chemical Oscillators. *Science* **323,** 614–617 (2009).

47. Golestanian, R. Collective Behavior of Thermally Active Colloids. *Phys. Rev. Lett.* **108,** 038303 (2012).